JOURNAL OF MATERIALS SCIENCE 11 (1976) 1667–1679

An electron microscopy study of the metastable structures in splat-cooled erbium–zirconium alloys

G. H. NARAYANAN, R. WANG*
Department of Materials Science, University of Southern California, Los Angeles, California, USA

The metastable structures produced by splat-cooling in Er–Zr alloys were investigated by using transmission electron microscopy and X ray analysis in order to deduce the mechanism by which a continuous series of supersaturated solid solutions are formed between Er and Zr in their low temperature h c p allotropic form. The study revealed that the microstructure of alloys with extended solid solubility consisted of an h c p phase exhibiting predominantly martensitic character together with small amounts of a metastable beta phase. The volume fraction of the martensitic phase increased and that of the beta phase decreased with increase in Zr content of the alloy. The phase transformations involved in the formation of the various metastable phases in the Er–Zr system during splat cooling and the stability of these phases during subsequent ageing treatments are discussed in relation to the equilibrium phase diagram for this system.

1. Introduction

The technique of rapidly quenching alloys directly from their melt, referred to as a splat cooling, is known to produce many unusual metastable phases, which represent radical departures from the equilibrium phases obtained by conventional alloy preparation techniques both in composition limits and crystal structures [1]. In many binary alloy systems, where only a limited terminal solid solubility is normally observed, splat cooling often extends the limits of the solid solubility significantly and in some cases produces complete miscibility.

The phase diagram for the Er–Zr system (Fig. 1) shows two principal terminal solid solutions – an Er-rich solid solution in the low temperature h c p allotropic form of Er (α_{Er}), and a Zr-rich solid solution in the high temperature b c c allotropic form of Zr (β_{Zr}) – separated by a simple eutectic [2]. At the eutectic temperature of 1450° C, a maximum of 27.3 at.% Zr is soluble in α-Er and approximately 48 at.% Er is soluble in β-Zr. The solubility of Er in α-Zr and that of Zr in β-Er are very restricted. In a recent investigation by Wang [3, 4] it was observed that a continuous series of solid solutions between Er and Zr in their low temperature h c p allotropic form can be produced by splat cooling of Er–Zr alloys. This was probably the first instance where metastable solid solutions have been obtained between two elements in their low temperature allotropic form by splat cooling. The formation of such metastable h c p solid solutions between Er and Zr seems highly unlikely from phase diagram considerations alone, since Er exhibits rather extensive solubility (~ 48 at.%) in β-Zr at higher temperatures, and negligible solubility (~ 2.8 at.%) in α-Zr at lower temperatures. This interesting result prompted the following systematic investigation of the metastable phases produced by splat cooling of Er–Zr alloys.

In the investigations of Wang [3, 4] X-ray diffraction analysis was used to determine the crystal structure of splat-cooled Er–Zr alloys and to

*Present address: Battelle Memorial Institute, Pacific Northwest Lab., Richland, Washington 99352, USA.

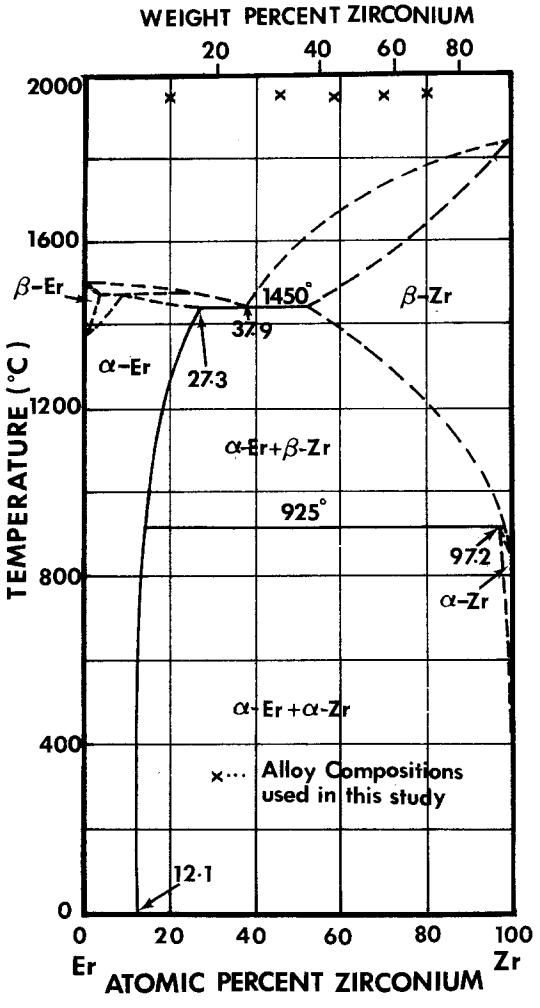

Figure 1 Equilibrium diagram for Er–Zr system according to Elliot [2].

identify the phases present. The lattice constants of the metastable Er–Zr solid solutions measured as a function of alloy composition (Fig. 2) show negative deviations from Vegards Law. The plot of lattice constants versus composition (Fig. 2) exhibit two minima occuring at ~ 41 and ~ 70 at. % Zr, which are separated by a hump. The occurrence of such a hump in an otherwise smooth variation of lattice constants with composition suggests existence of instabilities in the solid solutions of these compositions. X-ray analysis, however, failed to reveal the presence of a second phase in the splat-cooled alloys.

In the present investigation, thin foil transmission electron microscopy was used to ascertain the details of the microstructure of splat-cooled Er–Zr alloys. Structure determination and phase identification was carried out by using both X-ray and electron diffraction analysis. A study of the microstructural characteristics of the metastable phases produced by splat cooling and their stability during subsequent ageing would enable us to obtain information regarding the mechanisms by which such metastable solid solutions are formed in this system.

2. Experimental procedure

A series of Er–Zr alloys weighing about 2 g were prepared from 99.9 + % Er and 99.99% pure Zr by conventional arc melting techniques under purified argon atmosphere. The metastable solid solutions were obtained by splat cooling techniques originally developed by Duwez *et al.* [1]. Approximately 300 mg of the as-cast material was melted in a Zr-coated quartz crucible by induction heating and then atomizing by high pressure helium gas; the resulting droplets were impinged onto a copper substrate held at room temperature. The entire splat-cooling operation was done in argon atmosphere, details of the design of the splat-cooling apparatus is described elsewhere [3]. Since the weight loss during arc melting was always less than 0.5%, the splat-cooled alloys are referred to by their nominal compositions.

Isothermal ageing at temperatures below ~ 200° C was carried out in a constant temperature silicone oil bath. Specimens were wrapped in tantalum foils and sealed in vycor capsules under a vacuum of 10^{-6} Torr prior to heat-treatment. For higher ageing temperatures, muffle furnaces were used.

Many regions of the splat-cooled specimens were sufficiently thin and suitable for transmission electron microscopy without further specimen preparation. The thin foils were examined using Hitachi HU-125 electron microscope operated at 125 kV. Structural analysis by X-ray diffraction was done by a Gunier focusing camera using Cu$K\alpha$ radiation, and precision lattice parameters were measured by a GE XRD-6 diffractometer unit.

3. Experimental results

3.1. Microstructure of splat-cooled alloys

The transmission electron micrographs of splat cooled Er–Zr alloys, exhibited several common characteristic features irrespective of the alloy composition. The microstructures, in general, were composed of elongated grains, a few microns in width and several microns in length. Also evident in the micrographs was a high density of extinction

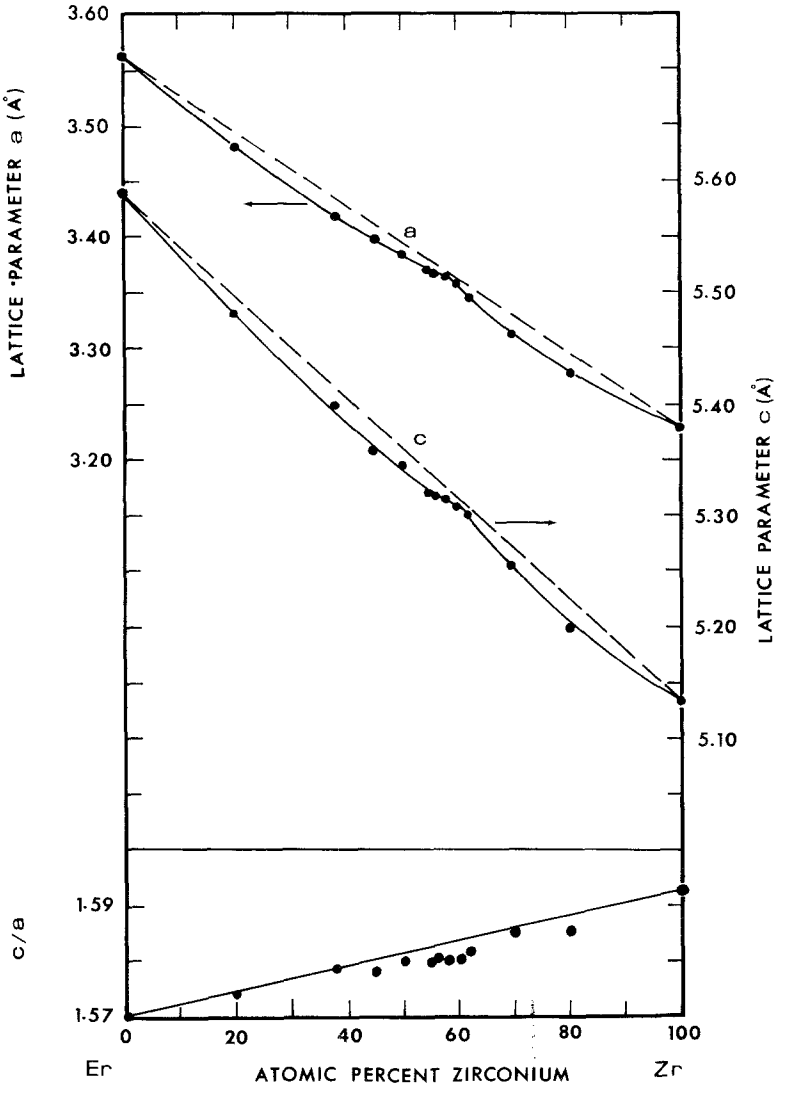

Figure 2 Lattice constants of metastable Er–Zr h c p solid solutions produced by splat cooling as a function of composition.

contours, which indicated that considerable internal strain was introduced in the material as a result of splat cooling. For an alloy of given compositions, thin foil specimens obtained from different regions of the splat-cooled material, exhibited variations in their microstructure. Such variations are believed to be caused by the differences in the cooling rates that prevailed in different parts of the splat-cooled alloy. Similar observations were reported by Stoering and Conrad [5] in a splat-cooled Ag–Cu alloys and by Furrier and Warlimont [6] in splat-cooled Al–Fe alloys.

Fig. 3 shows a typical bright-field micrograph taken from an Er–20 at.%* Zr alloy in the as-splat-cooled condition. Evident in this microstructure is a high density of twins. The selected-

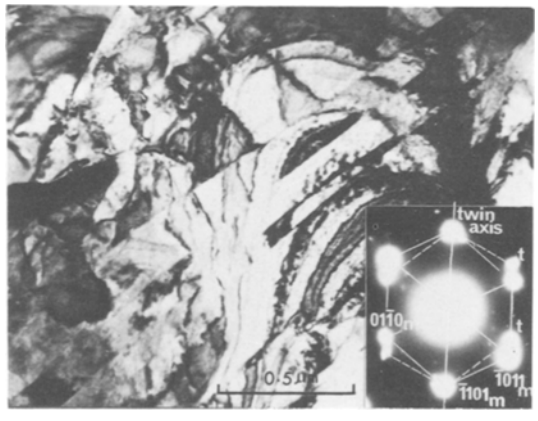

Figure 3 Bright-field electron micrograph of splat-cooled Er–20 at.% Zr alloy, showing a high density of twins Corresponding electron diffraction pattern is shown as insert.

*Note: henceforth all alloy compositions will be given in at.%.

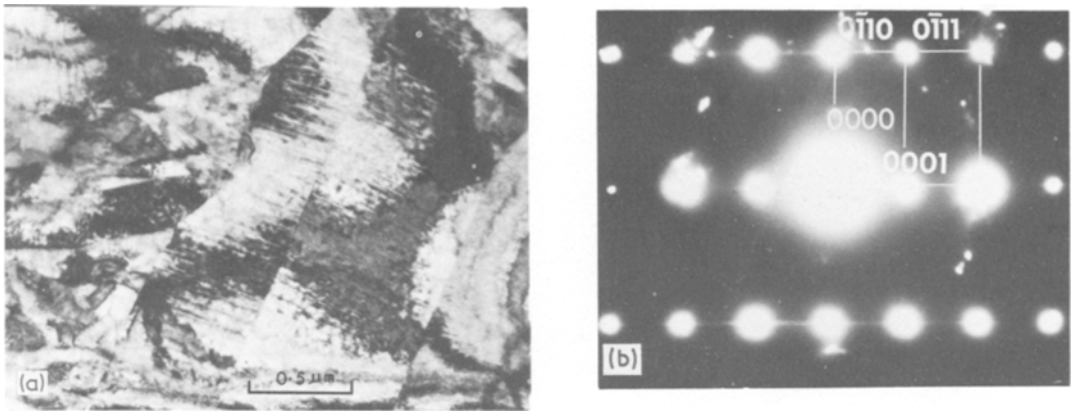

Figure 4 (a) Bright-field electron micrograph of splat-cooled Er–45 at.% Zr alloy showing martensitic microstructure (b) Selected-area electron diffraction pattern corresponding to the region in (a).

area electron diffraction pattern corresponding to this region (shown as an insert in Fig. 3) indicates that it is composed of a single h c p phase which is twinned about the $\langle \bar{1}\,1\,0\,1 \rangle$ crystallographic axis. Lattice constants of this phase estimated from the electron diffraction patterns ($a \approx 3.49$ Å and $c \approx 5.25$ Å) show good agreement with the values determined previously by X-ray analysis [3]. Examination of several thin foils taken from various parts of the splat-cooled material failed to reveal the existence of any other phases in this alloy.

With increase in the Zr content, the twin density in the splat-cooled alloy was found to decrease drastically. The microstructure of an Er–45 Zr alloy was virtually free of twin platelets of the type shown in Fig. 3. Electron micrographs taken from this alloy revealed two distinctly different types of microstructures depending on the specimen thickness. Relatively thin areas of the specimens exhibited morphological features which were largely martensitic in character. Fig. 4a shows a typical example of this type of microstructure. This region is composed of large lath type martensitic platelets which are aligned parallel to each other. Selected-area electron diffraction analysis (Fig. 4b) has shown that the structure of the martensitic phase is h c p and that all the platelets in Fig. 4a have the same crystallographic orientation. The average values of the lattice constants of this phase estimated from the electron diffraction patterns are: $a \sim 3.36$ Å and $c \sim 5.32$ Å. These values are slightly smaller than those determined previously by X-ray analysis [3] for the metastable solid solution of the same composition produced by splat-cooling. Also evident in the electron diffraction pattern (Fig. 4b) are streaks along the $\langle 0\,0\,0\,1 \rangle$ direction. The occurrence of these streaks indicates the presence of planar disorders on planes parallel to the basal plane. An examination of the bright-field image shown in Fig. 4a reveals that the martensitic platelets contain fine striations which are parallel to $\langle 0\,\bar{1}\,1\,0 \rangle$ and thus normal to the direction of the streaks. These striations are believed to be microtwins which are probably formed as a means to accommodate the transformation strains. The martensitically formed supersaturated h c p solid solutions will be henceforth designated by α'.

In addition to the martensitic h c p phase, thicker regions of the splat-cooled Er–45 Zr alloys contained a second type of h c p solid solution phase which exhibited a weak modulated microstructure. A typical example is shown in Fig. 5. Selected-area electron diffraction patterns corresponding to these regions revealed reflections

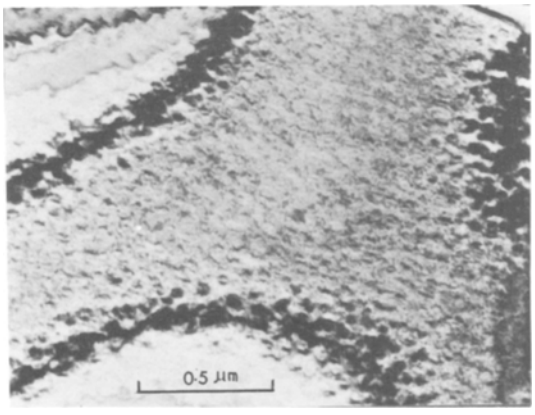

Figure 5 Weakly modulated microstructure in a splat-cooled Er–45 at.% Zr alloy.

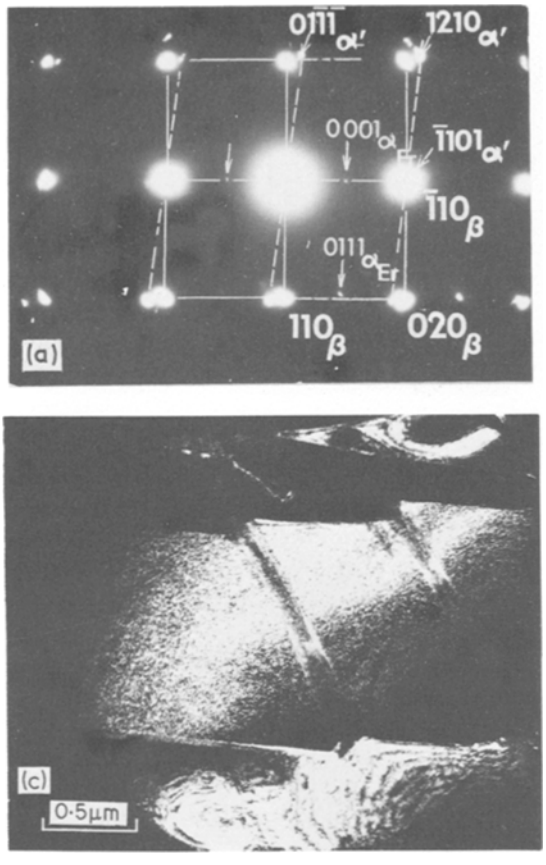

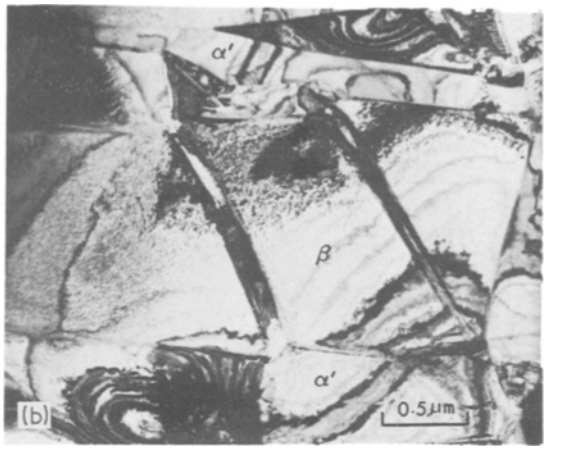

Figure 6 (a) Electron diffraction pattern taken from a splat-cooled Er–45 at.% Zr alloy showing the reflections from retained beta (b c c) phase superimposed on the pattern due to martensitic h c p phase (α'). (b) The bright-field micrograph corresponding to (a). (c) A dark-field micrograph obtained by imaging the $(1\,1\,0)_{\beta}$ reflection showing β-phase regions with precipitates.

due to only a single h c p phase, the lattice constants of which were slightly larger than those the martensitic h c p phase in this alloy. The spots in this pattern were, however, broadened but not streaked. It is believed that the modulations in the microstructure represent compositional instabilities in the metastable solid solutions. Henceforth, this metastable h c p phase will be designated by α_m. Similar modulated structures have been previously observed in splat-cooled Ag–Cu alloys also [5].

Although the X-ray powder diffraction patterns obtained from the splat-cooled Er–45 Zr alloy indicated the presence of only a single h c p phase, the selected-area electron diffraction patterns taken from isolated areas of the foils revealed, in addition, the existence of small amounts of a metastable b c c phase. Fig. 6a shows a typical example. The spots in this diffraction pattern can be indexed as those due to ⟨1 0 0⟩ oriented b c c phase superimposed on those due to a co-existing ⟨1 0 $\bar{1}$ 1⟩ oriented α'-phase. The lattice constants of this α'-phase was identical to that reported earlier while that of the β-phase was estimated to be ~ 3.71 Å. The overall microstructure of this region is shown in Fig. 6b. The identification of the α' and β regions in this micrograph was made by forming dark-field images of prominent α' and β reflections. Fig. 6c is a dark-field micrograph obtained by using the $(1\,1\,0)_{\beta}$ reflection in which the β-phase regions are resolved. It can be seen that the β-phase is internally twinned and contains a dispersion of fine precipitates. A careful examination of the diffraction pattern in Fig. 6a shows that, apart from the α' and β reflections, it contains additional faint spots which can be indexed as those due to a second h c p phase having ⟨$\bar{2}$ 1 1 0⟩ orientation. Lattice constants of this phase estimated from this pattern were much larger than that of the α' phase indicating that they must be richer in Er. The precipitates of this phase are resolved in Fig. 6c since the {1 0 $\bar{1}$ 0} reflection due to this phase nearly coincides with that of the $(1\,1\,0)_{\beta}$ reflection. It is believed that these Er-rich precipitates are formed by the partial decomposition of the β-phase during the quench.

Electron microscopy studies of splat cooled Er–58% and Er–70% Zr alloys showed microstructural features which were similar in many respects to those observed in the Er–45% Zr alloy. However, with increase in Zr content, there was a corresponding increase in the relative amount of the martensitic α' phase. In addition, the martensitic platelets exhibited a roughly acicular morphology. Fig. 7a shows a typical bright-field micro-

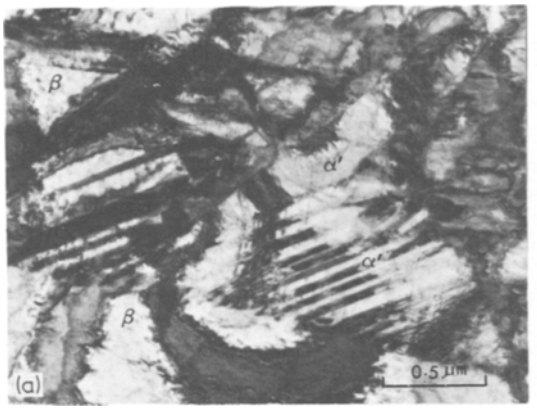

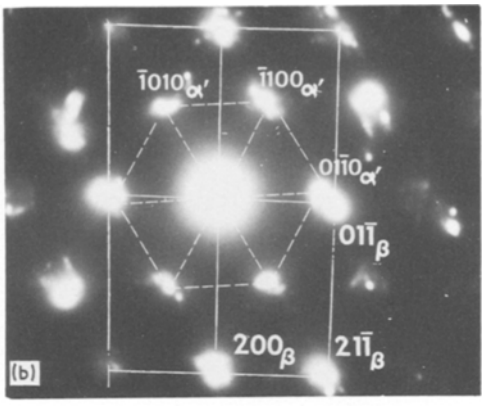

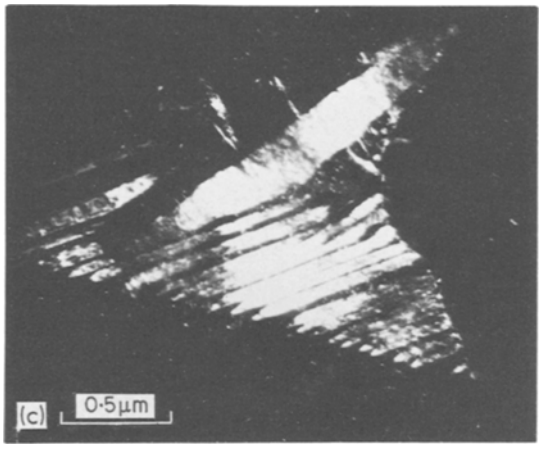

Figure 7 (a) Bright-field micrograph showing the microstructure of martensitically transformed regions in splat-cooled Er–58 at.% Zr alloy. (b) Selected-area electron diffraction pattern corresponding to the region in (a) showing the superimposed patterns from β and α' phases. (c) Dark-field micrograph obtained by imaging the $(1\,\bar{1}\,0\,0)_{\alpha'}$ reflection revealing the morphology of the martensitic α' phase.

graph illustrating the overall morphology of a martensitically transformed region in the Er–58% Zr alloy. The corresponding selected area diffraction pattern is shown in Fig. 7b. Dark-field microscopy was used to aid in the indexing of this pattern. A detailed analysis showed that this pattern is composed of the reflections from the $\langle 0\,0\,0\,1\rangle$ oriented α'-phase superimposed on the spot pattern due to the $\langle 1\,1\,0\rangle$ oriented β matrix. It can be seen that the martensitic α' phase maintains approximate Burgers orientation relationship with the β-phase, i.e. $\langle 0\,0\,0\,1\rangle_{\alpha'} \| \langle 1\,1\,0\rangle_{\beta}$ and $\langle 1\,1\,\bar{2}\,0\rangle \| \langle 1\,1\,1\rangle_{\beta}$ which is expected if the hcp phase is formed from the parent β phase. Fig. 7c is a dark-field micrograph obtained by imaging the $(1\,0\,\bar{1}\,0)_{\alpha'}$ reflection. The acicular morphology of the martensitic α' phase is clearly evident in this micrograph.

In addition to the α'-phase, the diffraction pattern in Fig. 7b also shows reflections from a second hcp phase also having $\langle 0\,0\,0\,1\rangle$ orientation but having lattice constants larger than those of α'.

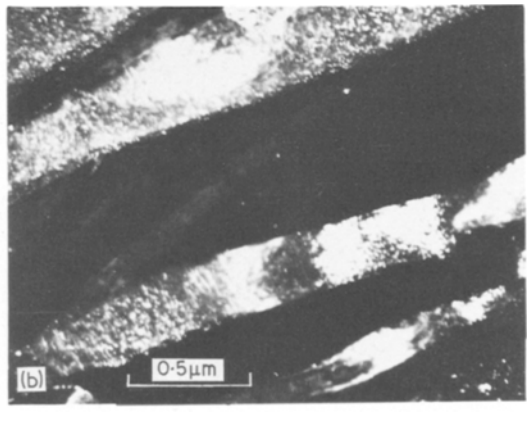

Figure 8 (a) Bright-field micrograph illustrating the microstructure of splat-cooled Er–80 at.% Zr alloy. (b) Dark-field micrograph corresponding to (a) showing precipitation within martensite platelets.

These are believed to be caused by Er-rich precipitates which result from the partial decomposition of the retained β-phase. This was confirmed by dark-field analysis, which revealed a dispersion of fine precipitate particles in the β-phase regions (Fig. 7c). As in the case of the splat-cooled Er–45% Zr alloy previously described, alloys containing 58% and 70% Zr also revealed the presence of non-martensitic h c p solid solution regions having a modulated structure.

The microstructure of splat-cooled Er–80% Zr alloy was composed almost exclusively of the martensitic h c p solid solution, α'. A typical example is shown in Fig. 8a. Unlike the alloys of lower Zr contents, there is clear evidence for the occurrence of a precipitation reaction within the martensitic platelets. By using selected-area electron diffraction analysis the precipitates were identified as those of an Er rich h c p phase. Fig. 8b shows a dark-field micrograph obtained by imaging a prominent precipitate reflection and reveals the precipitate particles, which are aligned roughly perpendicular to the long axis of the martensitic platelets. In addition to the martensitic α', small amounts of the retained β-phase was also detected in this alloy.

3.2. Annealing of splat-cooled alloys.

Splat-cooled Er–Zr alloys were isothermally annealed at temperatures in the range of ambient ($\sim$ 25° C) to 600° C to ascertain the stability of the as-quenched metastable structures and to establish the sequence of the decomposition reactions. Only alloys of compositions of 45, 58 and 70 at. % Zr were used in this study.

No change was detected in the microstructures of the as-quenched alloys up to a period of 30 days at room temperature. Upon annealing at 180° C and above, evidence for the initiation of a decomposition process was observed in the electron micrographs from all three alloys. The overall decomposition behaviour of the 45, 58 and 70 at. % Zr alloys during annealing was similar in most respects. Since the structure of the as-quenched alloys was composed of a mixture of the martensitic α', the weakly modulated α_m and retained β-phases, ageing characteristics of each of these phases will be treated separately.

3.2.1. Decomposition of the martensitic α'-phase

The decomposition of the martensitic α'-phase in splat-cooled Er–Zr alloys was found to be extremely sluggish at temperatures below $\sim$300° C. During annealing at 180° C, the boundaries of the internal microtwins became progressively sharper with annealing time. Annealing for a period of 250 h resulted in the appearance of pronounced strain field contrast parallel to these microtwin boundaries. A typical example for the case of Er–58% Zr alloy is shown in Fig. 9. The selected-area electron diffraction patterns corresponding to this region, however, did not show any evidence for the presence of a second phase. As will be shown later this sharpening of the microtwin boundaries and the subsequent development of strain-field contrast are the result of segregation of excess solute (Er in the present case) to these boundaries. Continued ageing at 180° C for periods in excess of 350 h did not produce any further change in the microstructure.

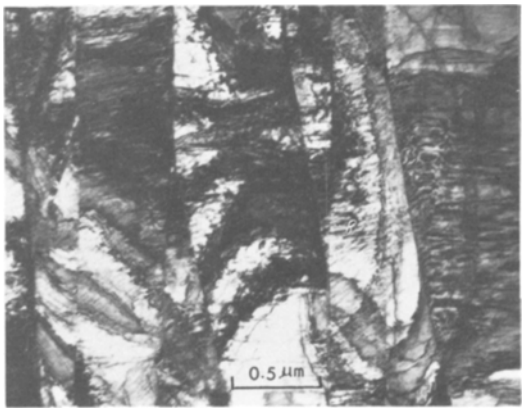

Figure 9 Microstructure of splat-cooled Er–58 at % Zr alloy following ageing at 180° C for 250 h showing sharpening of the microtwin boundaries.

When annealed at 250° C for 115 h, it was possible to detect the formation of thin plate-like precipitates parallel to the microtwin boundaries. The corresponding selected-area diffraction patterns revealed the presence of extra reflections which were displaced radially from the matrix spots towards the centre (Fig. 10a). An analysis of this pattern shows that the second phase has the same structure and orientation as the parent α'-phase and possesses lattice constants which are larger than those of α'. The precipitates are, therefore, believed to be those of the equilibrium α_{Er}-phase. A dark-field micrograph obtained by imaging a precipitate reflection is shown in Fig. 10b and reveals the precipitate platelets in contrast.

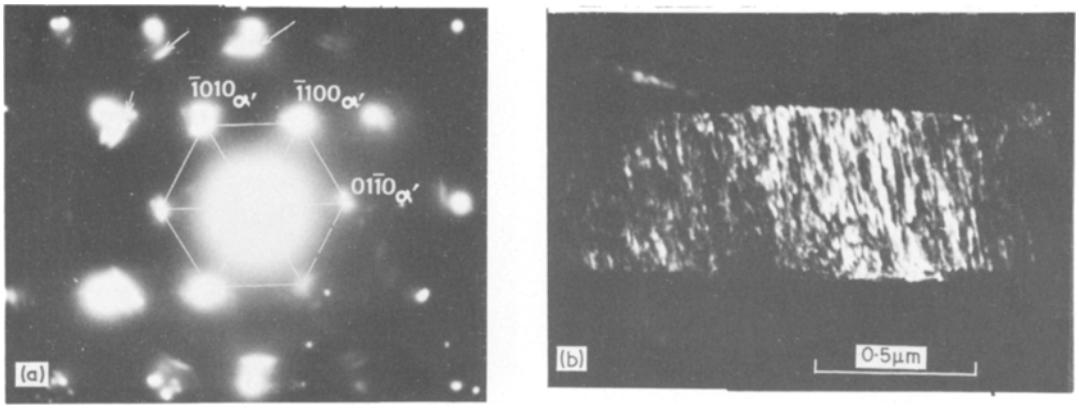

Figure 10 (a) Selected-area electron diffraction pattern from splat-cooled Er–58 at.% Zr alloy following 115 h annealing at 250° C. Note the presence of additional reflections radially displaced from the matrix spots towards the centre. (b) Dark-field micrograph obtained by imaging an extra reflection in (a) revealing precipitate platelets parallel to the microtwins within the martensite.

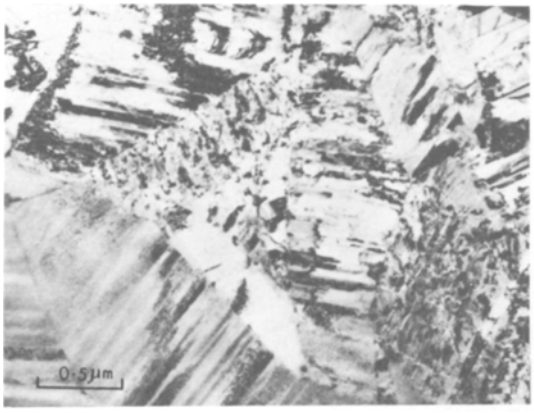

Figure 11 The microstructure of splat-cooled Er–58 at.% Zr alloy following 3 h annealing at 450° C showing the formation of second phase platelets.

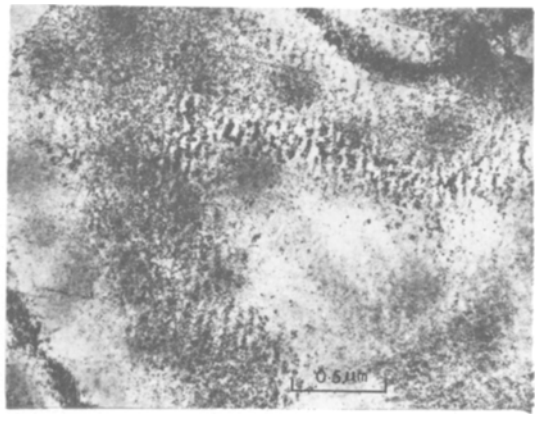

Figure 12 Bright-field micrograph showing sharpening of the modulated structure of splat-cooled Er–70 at.% Zr alloy following annealing at 180° C for 350 h.

During annealing at 350 and 450° C the kinetics of the martensite decomposition reaction was found to be significantly more rapid. Continued ageing at these temperatures resulted in the thickening of the precipitates platelets to develop a well defined lamaller structure. Fig. 11 shows resulting microstructure for the Er–158% Zr alloy following 3 h ageing at 450°C. The lattice constants of the parent α'-phase were found to decrease gradually with increase in annealing time suggesting that α' becomes progressively richer in Zr as the decomposition reaction proceeds.

3.2.2 Decomposition of weakly modulated α_m-phase

In the regions of the splat-cooled alloy, which exhibited a weak modulated h c p structure in the quenched state, the initial stages of decomposition during annealing at 180 and 250° C was marked by a sharpening of the modulations as shown in Fig. 12. The corresponding selected-area electron diffraction pattern, did not show any additional reflections due to a second phase. However, in many cases higher order reflections were split. This splitting is regarded as an indication of the formation of a precipitate phase which differ from the matrix only in its composition and hence in its lattice spacings. Annealing at 180° C for periods of time in excess of 350 h did not produce any further changes in the microstructure of the splat-cooled alloys. At 250° C, on the other hand, continued ageing resulted in the formation of a roughly columnar structure which evolved from the modulated microstructure. A typical example

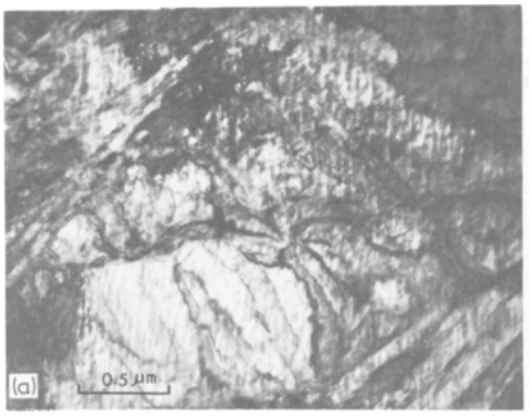

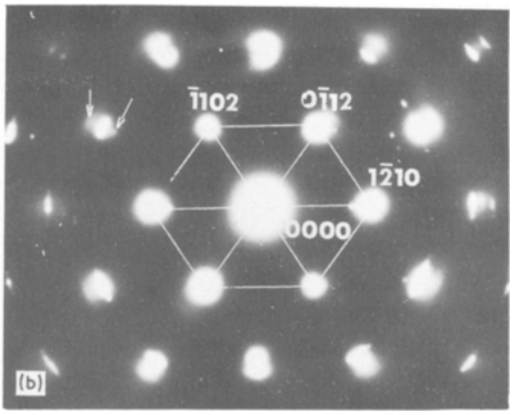

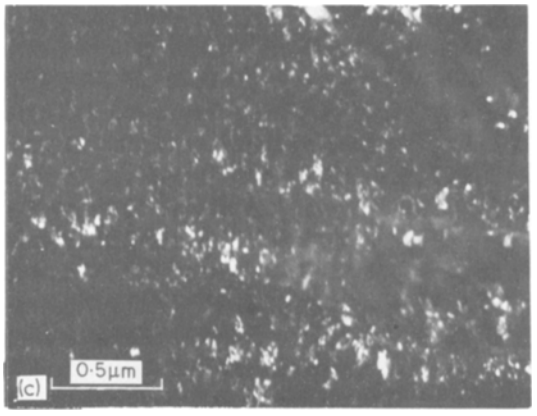

Figure 13 (a) Bright-field micrograph showing the development of a columnar-type structure in the same alloy as in Fig. 12 following annealing at 250° C for 350 h. (b) Selected-area diffraction pattern corresponding to the area in (a) showing the presence of extra reflections due to an Er-rich second phase (indicated by arrows). (c) A dark-field micrograph of the region in (a) obtained by imaging with an extra reflection showing the presence of precipitates.

of this type of microstructure for the Er–70% Zr alloy, aged at 250° C for 350 h and the corresponding selected-area diffraction pattern are shown in Fig. 13a and b respectively. In addition to the reflections from the parent h c p solid solution ($a \sim 3.31$ Å and $c \sim 5.20$ Å), a number of extra spots which can be indexed as those due to a second h c p phase having the same orientation but with larger lattice constants ($a \sim 3.48$ Å, $c \sim 5.44$ Å) than the matrix. Since the latter values of the lattice constants agree reasonably well with those for α_{Er}, the precipitate phase has been identified as the equilibrium α-Er. Fig. 13c is a dark-field micrograph obtained by imaging a prominent precipitate reflection and illustrates the ⟨0 0 0 1⟩ aligned morphology and distribution of the product phase.

As in the case of the martensitic α′ phase, the decomposition of the α_m phase was very sluggish at temperatures below ~ 300° C and did not go to completion even after ageing for 350 h. However, at 350, 450 and 600° C, the kinetics of the decomposition reaction was sufficiently rapid to allow near equilibrium structures to be formed within shorter periods of time. The decomposition of the metastable α_m-phase at these temperatures was found to proceed in a fashion similar to cellular or discontinuous precipitation [7]. The decomposition begins with the heterogeneous nucleation of a small colony or cell of the equilibrium α-Er and α-Zr phases at the grain boundaries and proceeds by the migration of the cell boundary into the untransformed regions, thus slowly consuming it. Fig. 14a shows a bright-field micrograph obtained from the Er–70% Zr alloy following annealing at 350° C for 115 h. Evident in this micrograph is the boundary of the α-Er + α-Zr cell region (region I) advancing into the untransformed matrix (region II). By using selected-area diffraction analysis it was confirmed that both regions I and II have the same crystallographic orientation. Diffraction pattern corresponding to the boundary region (Fig. 14b) shows that radially displaced on either side of the reflections from the parent h c p phase, there exist two additional sets of reflections, corresponding to the equilibrium phases α_{Er} and α_{Zr}. With increase in annealing time, α_{Er} and α_{Zr} reflections increased in their intensity while the matrix reflections decreased in their intensity. However, no noticeable shift in the position of these reflections occurred during prolonged annealing. Fig. 14c shows a dark-field micrograph

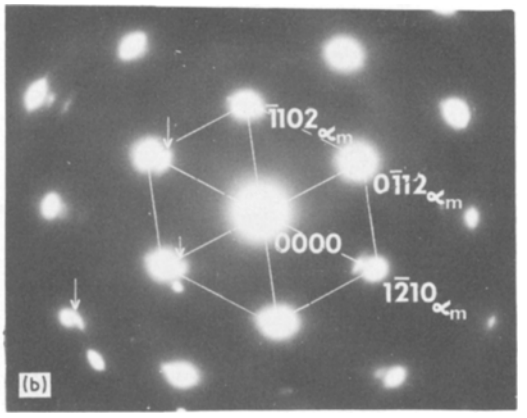

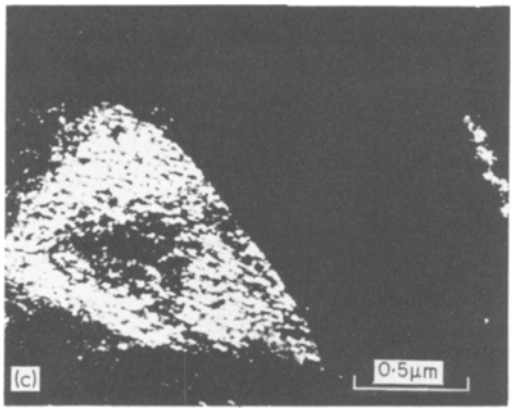

Figure 14 (a) Bright-field electron micrograph of a splat-cooled Er–70 at. % Zr alloy following ageing at 350° C for 115 h, showing boundary of region I advancing into region II during cellular decomposition reaction. (b) Selected-area diffraction pattern taken from the region near the boundary in (a). Notice the presence of two sets of additional reflections due to the equilibrium phases α_{Er} and α_{Zr}; one set radially displaced towards the inside and the other towards the outside of the α_m matrix reflections. (c) Dark-field micrograph obtained by imaging an α_{Er} reflection showing the distribution of α_{Er} precipitates in region I.

obtained by imaging a prominent α_{Zr} reflection (indicated by arrow in Fig. 14b) and reveals the morphology and distribution of the α_{Er} precipitates in the cellular-region. Similar decomposition behaviour was observed also in specimens annealed at 450 and 600° C.

The results of the X-ray diffraction analysis carried out on splat-cooled alloys in the middle of the composition range following high temperature annealing ($T > 300°$ C) were in general agreement with the electron microscopy observations. Powder X-ray diffraction patterns obtained from thick samples of the 45, 58 and 70 at. % Zr alloys indicated that isothermal annealing at 350, 450 and 600° C resulted in the simultaneous appearance of two sets of diffraction lines which lie on either side of the lines due to the parent solid solution. The lattice constants of these new phases were close to those expected for the equilibrium α_{Er} and α_{Zr} phases. It was found that the precipitation of the equilibrium phases did not cause any appreciable shift in the angular positions of the matrix diffraction lines. As decomposition proceeds the intensity of the lines due to the product phases increases and that of the parent phase decreases without there being any significant change in their relative positions. These observations indicate that during the decomposition only the relative volume fractions of the parent and product phases vary and no continuous changes in the composition (and hence in the lattice constants) occur in the parent phase. This is consistent with the behaviour expected during a cellular or discontinuous precipitation reaction.

4. Discussion

The results of the electron microscopy studies clearly demonstrate that the microstructure of splat-cooled Er–Zr alloys are more complex than what was originally inferred from X-ray diffraction analysis. In what follows we shall examine the phase structure of the different splat-cooled alloys in relation to the Er–Zr equilibrium phase diagram (Fig. 1) and propose a probable mechanism by which continuous series of solid solutions are formed between Er and Zr in their low temperature h c p allotropic form, during splat cooling.

The formation of a single supersaturated h c p solid solution, in the case of the splat-cooled Er–20% Zr alloy is not surprising, since according to the phase diagram an h c p solid solution of this composition is stable at elevated temperatures can

be formed directly from the melt during solidification. By rapid quenching this phase can be retained at room temperature in the metastable state. The formation of the h c p solid solutions with extended solubility in the case of the Er–45, 58, 70 and 80 at.% Zr alloys, on the other hand, does not seem feasible from phase diagram considerations alone. However, microstructural studies have revealed that in all cases where extended solid solubility was observed, the metastable h c p solid solutions exhibit a strong martinsitic character. Since martensitic structures can result only from a solid state phase transformation of the diffusionless-type, it follows that splat-cooling of the above alloys should involve initially the formation of an unstable high temperature phase, which during cooling to room temperature transforms to the low temperature allotropic form. An examination of the phase diagram shows that in the above alloys, with the exception of the Er–45% Zr alloy, solidification of the melt can initially produce a b c c (β) solid solution the same composition, which is stable at high temperatures. Rapid quenching of this phase to room temperature leads to a martensitic reaction, which produces an h c p solid solution having the same composition. The fact that small amount of the retained beta phase was detected in all the alloys with Zr content in excess of 40% and that the martensitic h c p phase maintained Burgers orientation relationship with the β-phase support the above suggestion. Even in the case of the Er–45% Zr alloy, it is reasonable to assume that splat-cooling extends the solubility of Er in β-Zr beyond the equilibrium value (48 at.% Er at the eutectic temperature, ~ 1480° C) so that a single b c c phase can be formed immediately upon freezing. The extended solid solubility in the h c p phase observed at room temperature can, thus, be regarded as a direct consequence of the extended solubility in the high temperature β-phase and the subsequent occurrence of the martensitic transformation.

As for the martensitic phase transformation, it is well known that in Zr and its dilute alloys with transition metal elements, b c c $\rightarrow$ h c p transformation occurs by a martensitic reaction when quenched rapidly from the β-phase field to room temperature [8]. It is reasonable to assume that a similar transformation might occur in alloys of Zr with rare earth elements also. The probability of the occurrence of the $\beta \rightarrow \alpha'$ martensitic transformation in splat-cooled Er-Zr alloys would be enhanced further by the fact that specimens produced by splat cooling are, in general, extremely thin. It is well known that the constraints to a shear transformation are negligible in thin foil specimens as compared to those present in bulk crystals so that there can be a significant reduction in the non-chemical component of the free energy change associated with the transformation [9, 10]. As a result, the M_s (martensite start) temperature in thin foils will be raised well above that for a bulk crystal. The high degree of internal stresses introduced as a result of rapid quenching from liquid state may also provide additional driving force for the shear transformation in the present case.

The variations in the microstructures of samples taken from a different area of a given splat-cooled alloy, can probably be rationalized on the basis of the differences in the cooling rates which prevail in different regions of a splat-cooled alloy. As has been pointed out by Duwez [11], the cooling rates achieved during splat cooling are inversely related to the specimen thickness. A two-fold increase in specimen thickness is equivalent to a ten-fold decrease in cooling rate. Consequently, in relatively thicker regions of the specimen where the cooling rates are low particularly for alloys in the middle of the phase diagram, solidification of the melt may lead to the formation of a mixture of supersaturated α- and β-phases at high temperatures rather than all beta.

On cooling down to room temperatures at rates below the critical value required for the martensitic transformation to occur, these phases may decompose by a diffusional reaction. The h c p solid solution having the modulated structure is believed to be the product of such a reaction.

The ageing studies on splat-cooled Er–Zr alloy have shown that the metastable structures produced by splat-cooling remain stable for prolonged periods at temperatures below ~ 200° C. At higher temperatures, however, both the martensitic α' and the modulated h c p solid solution α_m decompose into equilibrium α_{Er} and α_{Zr} phases. The decomposition of the martensitic α'-phase is similar in many respects to the tempering reaction observed in hexagonal martensites in many Zr and Ti alloys [8, 12]. In all these cases the twin interfaces are known to provide effective heterogeneous nucleation sites for the equilibrium phase (α_{Er} in the present case) which form as thin platelets parallel to these interfaces. The precipitation

of Er-rich α_{Er}-phase causes the remaining matrix to become progressively enriched in Zr and thus transform to α_{Zr}.

The spinodal type of decomposition reaction observed during low temperature ($T < 300^\circ$ C) ageing of α_m-phase is not surprising since the product phases α_{Er} and α_{Zr} differ from the parent phase only in their composition. However, owing to the large differences in the lattice constants of the α_{Zr} and α_{Er} phases (i.e. large misfit strain) a true spinodal decomposition probably does not occur in the present case (no side band structure was observed in the diffraction pattern). The phase separation occurs instead through a nucleation and growth process.

Both the X-ray diffraction and electron microscopy results indicate the occurrence of a cellular or discontinuous precipitation reaction during ageing at or above 350° C. It is known that in many age-hardening alloys (e.g. Al–Ag and Fe–Mo) discontinuous precipitation reaction occurs at later stages of ageing during which equilibrium phases are formed from metastable phases [13, 14]. The driving force for the migration of the boundary of the cell consisting of the equilibrium phases into the untransformed parent phase can be purely chemical or also due to strain energy effects. The latter is known to play a role when precipitation occurs from supersaturated solid solutions in which the solute atoms greatly differ in size from that of solvent atoms. It is evident that both types of driving force exist in the case of splat-cooled Er–Zr alloys. The fact that higher ageing temperatures promote rapid diffusion and interface mobility probably explains why the cellular decomposition reaction is observed only at these temperatures.

5. Conclusions

(1) The electron microscopy studies of the splat-cooled Er–Zr alloys over the entire composition range have shown that the microstructure of alloys having higher Zr content is composed predominantly of a supersaturated h c p solid solution phase exhibiting largely martensitic character and also of small amounts of retained β-phase.

(2) Since the martensitic phase can result only through a diffusionless solid state shear transformation from a high temperature unstable phase, it is proposed that the formation of the continuous series of supersaturated solid solution in the low temperature h c p allotropic form, during splat cooling involves initially the formation of a metastable b c c phase.

(3) The extended solid solubility of the h c p phase is thus a consequence of the extended solid solubility in the high temperature β-phase and the subsequent martensitic transformation of β to form α of the same composition.

(4) The variations in the microstructure of different parts of a given foil have been rationalized on the basis of the variations in the cooling rates which prevails in different regions of the foils as a result of the variations in sample thickness.

(5) On the basis of the present study we propose the following sequence of transformations during splat cooling and subsequent isothermal annealing:

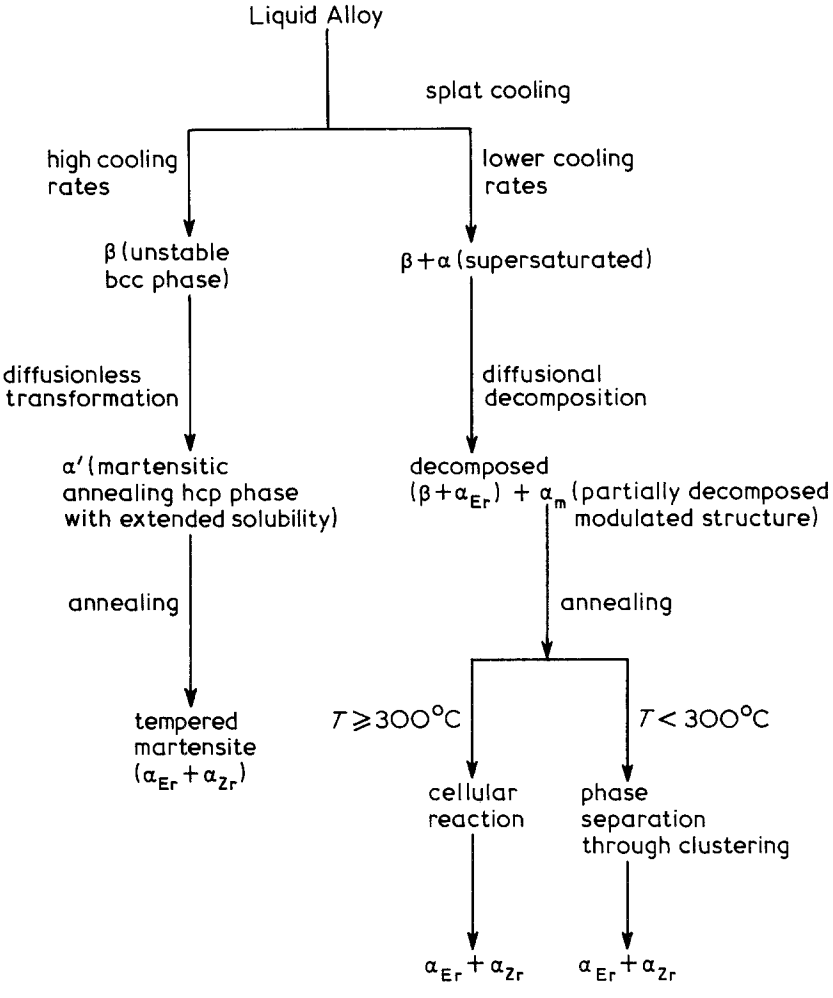

References

1. P. DUWEZ and R. H. WILLENS, *Trans. Met. Soc. AIME* **227** (1963) 362.
2. R. P. ELLIOT, "Construction of Binary Alloys", 1st Supplement (McGraw-Hill, New York, 1965) p. 409.
3. R. WANG, *Appl. Phys. Letters* **17** (1970) 460.
4. *Idem, Met. Trans.* **3** (1972) 1213.
5. R. STOERING and H. CONRAD, *Acta met.* **17** (1969) 933.
6. P. FURRER and H. WARLIMONT, Proceedings of the 7th International Conference on Electron Microscopy, Grenoble, France (1970) p. 507.
7. D. TURNBULL and K. N. TU, "Phase Transformation" (American Society for Metals, Metals Park, 1970) p. 487.
8. D. J. COMETTO, G. L. HOUZE and R. F. HEHEMANN, *Trans. Met. Soc. AIME* **233** (1965) 30.
9. W. PITSCH, *J. Inst. Metals* **87** (1958–59) 444.
10. D. HULL, *Phil. Mag.* **7** (1962) 537.
11. P. DUWEZ, *ASM. Trans. Quart.* **60** (1967) 607.
12. J. C. WILLIAMS, "Titanium Science and Technology", Vol. 3, edited by R. I. Jafee and H. M. Butte (Plenum, New York, 1974).
13. R. B. NICHOLSON and J. NUTTING, *Acta Met.* **9** (1961) 332.
14. Y. MURAKAMI and O. KAWANO, *Mem. Fac. Kyoto Univ.* **21** (1959) 393.

Received 31 December 1975 and accepted 9 February 1976.